

## Estimating Leaf Bulk Density Distribution in a Tree Canopy Using Terrestrial LiDAR and a Straightforward Calibration Procedure

### Supplementary A. Inventory-Based Method to Estimate Leaf Bulk Density Profiles and Loads in *Quercus pubescens* Plots: Equations Derivation

#### Description of the Inventory-Based Method

Eleven *Quercus pubescens* covering the Diameter at Breast Height (DBH) range found in Plots 1 to 4 were selected on the study site for destructive sampling. DBH, height and crown base height were recorded for each sampled stem that was felled and cut into 1-m sections. The various crown materials in each section were then separated by leaf and roundwood diameter size classes (0–6 mm, 6–25 mm and more than 25 mm). Leaves and twigs <25 mm in diameter were bagged up in the field, shipped to the laboratory, oven-dried at 60 °C for 24 hours, and weighed. Larger roundwoods were weighed fresh in the field and samples taken from three different sections were shipped to the laboratory for measurements of water content to estimate dry weight.

The dry weights of the various crown components were regressed against DBH using a power fit (Figure S1a for leaves). Cumulative mass profiles were constructed to quantify the vertical distribution of the material from individual trees in relation to relative height in crown (Figure S1b for leaves).

The stem inventories for each plot (tree DBH and heights), and the equations for individual leaf mass and distribution (Figure S1), were used to estimate the leaf bulk density profiles of Plots 1 to 4 (Figure 7, “crosses”) using the inventory-based method.

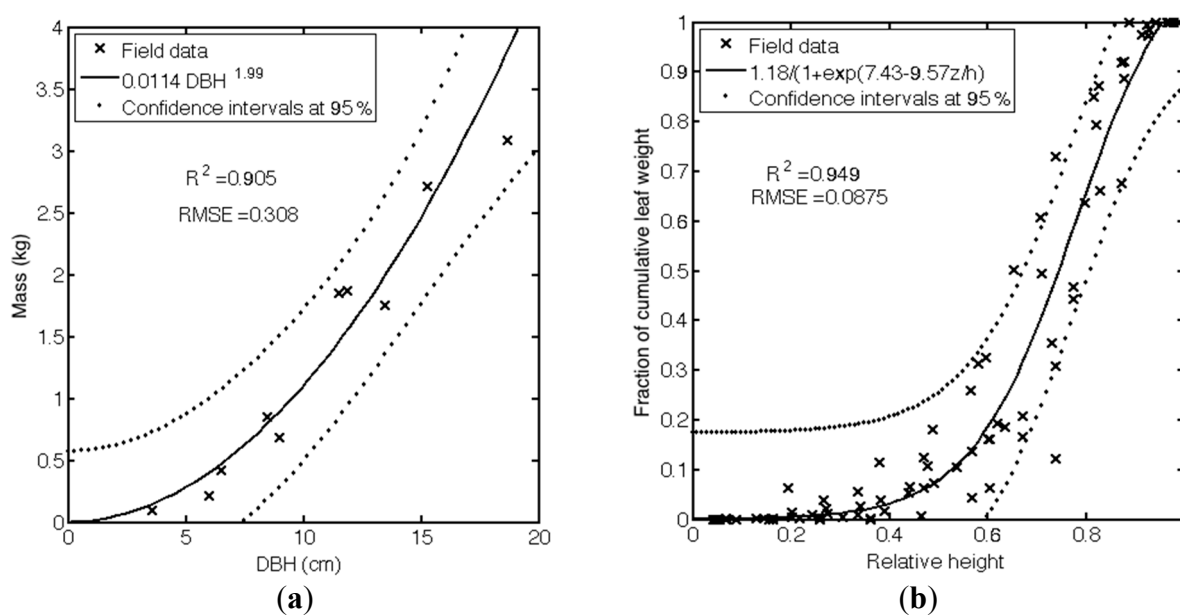


**Figure S1.** Equations for estimating individual tree leaf bulk density: (a) Allometric equation for tree leaf mass and (b) cumulative leaf weight distribution.

Regressions were done using package *nlinfit* of the MATLAB and Statistics Toolbox Release 2013b (The MathWorks, Inc., Massachusetts, United States). For the mass allometry, the sampled trees were weighed according to the distributions of trees in Plots 1 to 4, so that the inventory-based approach provides the most accurate estimations of biomass for these plots.

Similar work was performed on roundwoods  $>25$  mm and was used to compute the fraction of wood in the plot that was greater than a given height. These fraction profiles are plotted in Figure S2. This fraction decreased with height in canopy from 1 at  $z = 0$  m (all the wood was above 0 m) to 0 at the height at which no large wood was located. These functions were useful to determine below which height this absence of a separation between leaf and wood returns was likely to raise problems in the Terrestrial LiDAR System-based method that is the core of this paper.

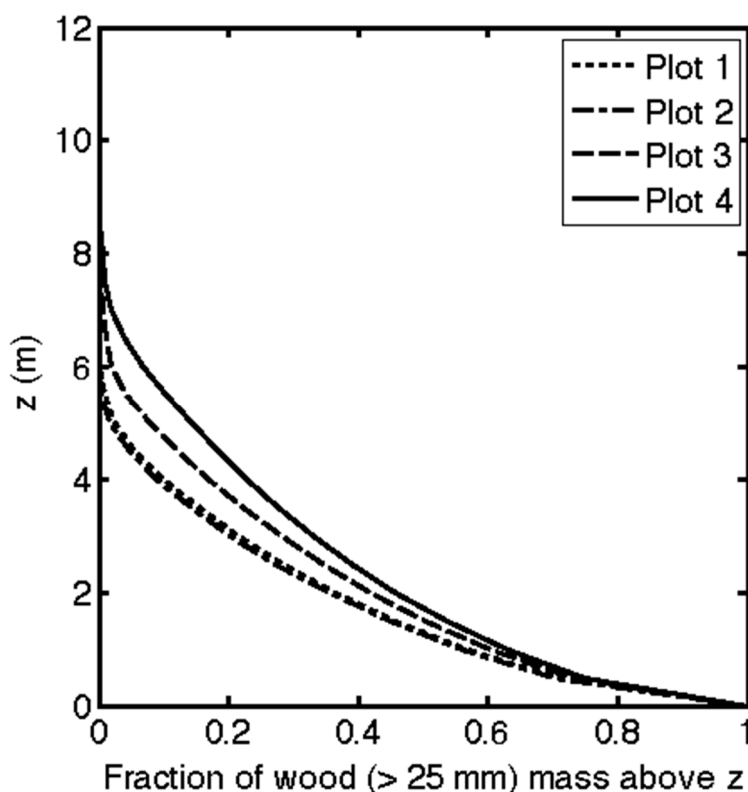


**Figure S2.** Fraction of the mass of wood (diameter greater than 25 mm) above a given height  $z$ .

#### *Limitations of the Inventory-Based Method in our Study*

The first limitation of the inventory-based method is its labor cost. On average, felling and 1-m cutting require the work of three persons for a day. The oven-drying period varies between two days for leaves and small twigs, and six days for thicker twigs. The labor cost associated with separation in element classes, drying and weighing is on the order of two persons for four to five days. Ten trees being the minimal number of trees for parameter estimation, the total cost to get accurate allometric equations is larger than 100 days of labor. Once the estimation of allometric equations is done, inventorying a new plot (measuring of DBH and height of about fifty trees) requires four hours of work (two persons for two hours).

The second limitation is its sensitivity on small plots due to the role played by uncharacteristic trees. In addition, individual tree biomass decreases with stand basal area [14] and our simple biomass equations did not take this into account. Thus, it is reasonable to assume that biomasses estimated by the inventory method were slightly underestimated in Plot 1 (low basal area) and slightly overestimated in Plot 4 (high basal area). The bulk density profiles and loads derived from the inventory may be considered to be reasonable estimates, but not a direct measurement of biomass. The hypothesis that biomass is overestimated by the inventory method in Plot 4 was consistent with the TLS-derived prediction that was slightly lower in Plot 4. The Weibull distribution used in the biomass distribution model may also induce underestimated predictions in the lower part of the canopy [13].

### Supplementary B. Recovering Information on Filtered Points

Computation of the indices, as described in Section 2.4, requires an estimation of (i) the number of points emitted in a given cone and filtered  $N_n$  (for  $N_t$  estimation), and (ii) the fraction of filtered returns that were specifically filtered by “Clear Contour” (to estimate  $f_{cc}$ ). Because the filtering in our study was operated by the scanner, no data were available in the output format of the FARO Scene software concerning either the emission direction of the filtered points or the type of filter responsible for it. However, the Cyclone point cloud export format (“.ptx”) can be used to make this information available [1]. In this format, FARO SCENE prints the point coordinates in order of acquisition by half hemisphere, from ground to vertical. Filtered points have 0, 0, 0 coordinates but the emission direction can be estimated from neighboring unfiltered points in the file. Unit vectors corresponding to emission direction can thus be computed for each filtered point. This recovery of filtered direction is illustrated in Figure S3, which shows the fraction of points filtered in each elementary angle ( $1^\circ \times 1^\circ$ ) in spherical coordinates. The transformation matrix provided in the file is used to compute coordinates in the common Cartesian system. The unit vectors associated with the emission directions of filtered beams were used to compute  $N_n$  (and thus  $N_t$ ) for each spherical volume (for calibration or model application).

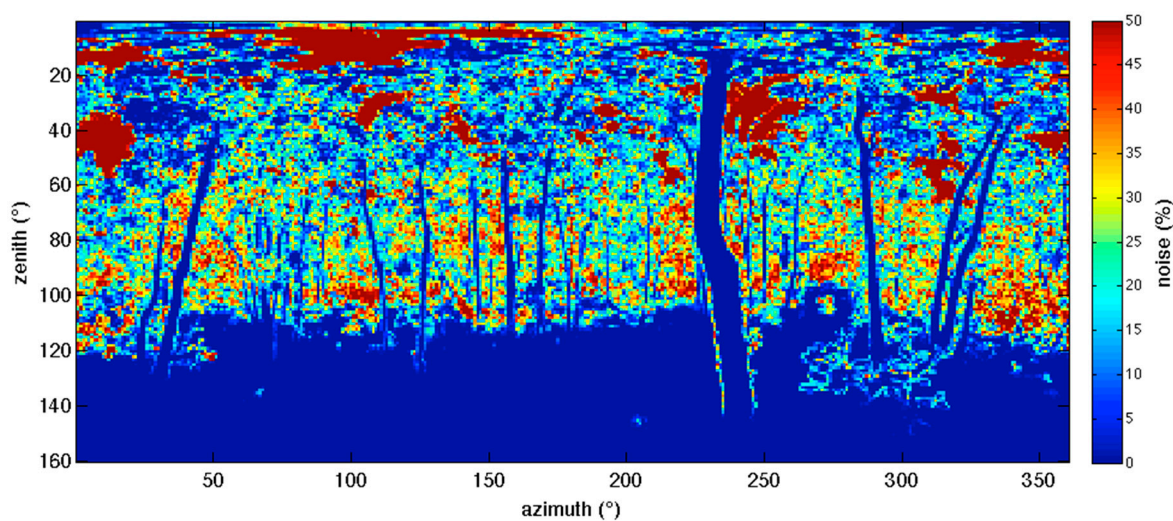


**Figure S3.** Percentage of filtered returns in a  $1^\circ$  pixel.

In Figure S3, the returns filtered by “Clear Sky” (in canopy gaps) have a high filtering percentage in each  $1^\circ$  pixel (greater than 50%), whereas the returns filtered by “Clear Contour” (mixed-points near

trunks or in foliage) generally have a lower filtering percentage. This property was used to develop a criterion for discriminating returns filtered by “Clear Sky” and “Clear Contour”. Three additional scans with both filters, “Clear Sky” only or “Clear Contour” only were performed and compared to fit a logistic regression used to predict if a filtered return was filtered by “Clear Sky” or “Clear Contour”, in relation to the percentage of filtered returns in the surrounding  $1^\circ$  pixel ( $P_f$ ).

$$P(P_f) = \frac{1}{1 + e^{4.73 - 0.0839P_f}} > 0.5 \quad (\text{B1})$$

This criterion can be used to discriminate the type of filter used by the scanner to filter returns with a 92.3% success.

### Supplementary C. Example of New Metric for Crown Fire Prediction

The probability of transition from surface to crown fire in conifer forests depends on some bulk density thresholds and decreases with crown base height [2,3]. However, these common metrics do not account for horizontal continuity between fuel clumps, which is also known as a factor for transition from surface to crown fire. 3D distributions of leaf bulk density estimated with TLS can be used to compute new metrics based on the percentage of the canopy volume in which a fire can spread. Here, we propose to compute for each height  $z$ , the percentage of canopy volumes with higher density than a combustibility threshold (e.g. below with  $0.1 \text{ kg}\cdot\text{m}^{-3}$ ). Depending on other fuel and ambient conditions, like fuel moisture and wind speed, a crown fire could appear only when this percentage is higher than a threshold, below a given height. This metric combines fuel density, fuel height and canopy structure. The threshold values could be determined with experiments or simulations. Figure S3 shows the vertical profile of the percentage of canopy volume occupied by more than  $0.1 \text{ kg}\cdot\text{m}^{-3}$ .

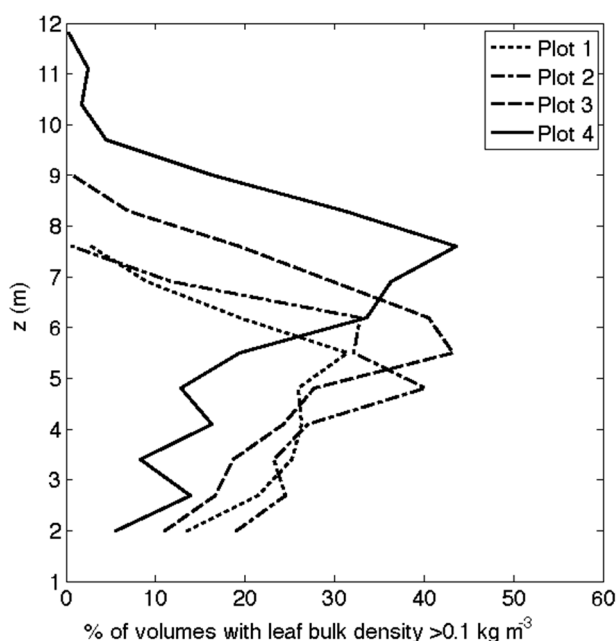


**Figure S3.** Profile of the percentage of canopy volume with fuel denser than  $0.1 \text{ kg}\cdot\text{m}^{-3}$ .

## References

1. Cyclone Pointcloud Export Format—Description of ASCII.ptx Format. Available online: <http://www.leica-geosystems.com/kb/?guid=5532D590-114C-43CD-A55F-FE79E5937CB2> (accessed on 10 June 2015).
2. Ruel, J.J.; Ayres, M.P. Jensen's inequality predicts effects of environmental variation. *Trends Ecol. Evol.* **1999**, *14*, 361–366.
3. Béland, M.; Widlowski, J.-L.; Fournier, R.A. A model for deriving voxel-level tree leaf area density estimates from ground-based LiDAR. *Environ. Model. Softw.* **2014**, *51*, 184–189.

© 2015 by the authors; licensee MDPI, Basel, Switzerland. This article is an open access article distributed under the terms and conditions of the Creative Commons Attribution license (<http://creativecommons.org/licenses/by/4.0/>).